

HEAT CAPACITY AT CONSTANT PRESSURE AND THERMODYNAMIC PROPERTIES OF PHASE TRANSITIONS IN PbMO_3 ($M=\text{Ti, Zr AND Hf}$)

T. Yoshida¹, Y. Moriya², T. Tojo¹, H. Kawaji^{1,*}, T. Atake¹ and Y. Kuroiwa³

¹Materials and Structures Laboratory, Tokyo Institute of Technology, 4259 Nagatsuta-cho, Midori-ku, Yokohama 226-8503, Japan

²Department of Chemical System Engineering, The University of Tokyo, 7-3-1 Hongo, Bunkyo-ku, Tokyo 113-8656, Japan

³Department of Physical Science, Graduate School of Science, Hiroshima University, 2-313 Kagamiyama, Higashi-Hiroshima 739-0046, Japan

The heat capacity of PbMO_3 ($M=\text{Ti, Zr and Hf}$) at constant pressure was measured using a differential scanning calorimeter (DSC) from room temperature up to 870 K. Large anomalies were found in the heat capacity curves, corresponding to the ferroelectric-paraelectric phase transition in PbTiO_3 (PT), the antiferroelectric-paraelectric phase transitions in PbZrO_3 (PZ) and PbHfO_3 (PH). The transition entropies were estimated as $7.3 \text{ J K}^{-1} \text{ mol}^{-1}$ (PT), $9.9 \text{ J K}^{-1} \text{ mol}^{-1}$ (PZ) and $9.3 \text{ J K}^{-1} \text{ mol}^{-1}$ (PH). These values of transition entropies are much larger than that of a typical displacive-type phase transition.

Keywords: DSC, heat capacity, PbHfO_3 , PbTiO_3 , PbZrO_3 , phase transition

Introduction

Perovskite oxides represented as ABO_3 are scientifically and technologically important materials because of their high potentiality in application of ferroelectric and piezoelectric properties. Most of the perovskite oxides are of cubic structure (space group: $Pm\bar{3}m$) at high temperatures and often have a variety of lower-symmetry phases at low temperatures. In the case of $A=\text{Pb}$, that is PbBO_3 , a variety of properties are observed depending on the B -site cation. For example, PbTiO_3 (PT) shows a ferroelectric phase transition at 763 K and the low temperature phase is tetragonal ($P4mm$) [1]. On the other hand, PbZrO_3 (PZ) shows an antiferroelectric phase transition at 503 K. PbHfO_3 (PH) has two-phase transitions at 433 and 476 K [2, 3]. The low temperature phase of PZ is antiferroelectric and of orthorhombic ($Pbam$) symmetry, which is isomorphous with the lowest temperature phase of PH below 433 K. The intermediate phase of PH is also antiferroelectric [4, 5] and the symmetry of the intermediate phase belongs to one of the space groups $P222_1$, $Pmm2$, $Pmmm$, or $P222$ [6, 7].

Although many studies have been made on the phase transitions in these perovskite materials, the mechanism has long been in controversy between displacive-type and order-disorder-type. The phase transition in PT has been considered to be of a displacive-type [8, 9], but recently an order-disorder nature has been reported [10–13]. There have been also similar reports on PZ and PH [14–16]. Although there have been several reports on the heat capacity of

PT and PZ [1, 2, 17–20], some disagreements are among them. Furthermore, no report is given on the heat capacity of PH. The heat capacity measurement occupies an important position in such studies on material properties. In the present study, heat capacity measurements were made for PbMO_3 ($M=\text{Ti, Zr and Hf}$) at constant pressure by differential scanning calorimetry (DSC) from room temperature up to 870 K. For the measurement of PH below room temperature, a relaxation-type calorimeter was used. We provide another insight into the phase transition mechanism of PT, PZ and PH, on the basis of the results of the present heat capacity measurements.

Experimental

Powder samples of PT, PZ and PH were prepared by solid-state reaction methods. Starting materials of PbO (99.99%), TiO_2 (99.99%), ZrO_2 (99.99%) and HfO_2 (99.95%) were purchased from Rare Metallic Co., Ltd., Japan. The materials were weighed in the stoichiometric ratio and then mixed in an alumina mortar with ethanol, where 3 mol% excess PbO was added to avoid lead-loss during the reaction process. These mixtures were put into a platinum crucible and then heated at 900°C for 12 h. The resultant powder was pressed into pellets of 14 mm in diameter and 2 mm in thickness. These pellets were sintered at 1000°C for 1 h. It was confirmed by X-ray powder diffractometry that all the samples were of single perovskite phase.

* Author for correspondence: kawaji@msl.titech.ac.jp

In the high temperature region from room temperature up to 870 K, heat capacity measurements were made using a power-compensation differential scanning calorimeter (Pyris 1 DSC; Perkin-Elmer, Inc., USA) for all the samples. The heat capacity was measured by so-called enthalpy method (step-scanning method) [21]. The temperature indicated by the instrument was calibrated with the melting and phase transition temperatures of standard materials (indium, tin, bismuth, lead, zinc and lithium sulphate) at different heating rates [22, 23]. In the enthalpy method, the correction was made at 0 K min⁻¹, i.e., an isothermal state, by extrapolating the difference between the indicated and reference temperatures as a function of heating rate to 0 K min⁻¹. During the measurements, nitrogen gas-flow was kept at a constant flow rate of 20 mL min⁻¹. A sequence of measurements was carried out on three different aluminum pans of the same mass under the same conditions, where each pan included no sample (blank run), α -Al₂O₃ (reference run; standard material for the enthalpy calibration [24]; Rare Metallic Co., Ltd., 99.999%) and sample (sample run). The calorimeter cell was kept at the initial temperature for 5 min in order to get an isothermal baseline and then it was heated up to the final temperature. At the final temperature, the cell was kept for 5 min. In the present study, the measurements were made with heating periods of 5 K increment at 5 K min⁻¹ heating rate. Since the calorimeter conditions are changeable as time goes by, the measurement was divided into several temperature segments with 100~150 K intervals to minimize the influence of change of the calorimeter conditions and a sequence of the three runs was made in each segment.

DSC data were collected as a function of time. The area between the actual DSC curve and the baseline is proportional to the enthalpy increment of the sample between the initial and final temperatures. The baseline was obtained by interpolation between the isothermal baselines at the initial and final temperatures. This procedure was performed on the three runs. The enthalpy change of the sample (and the standard) was calculated by subtracting the integrated area of the blank run from that of the sample run (and the standard run). The enthalpy increment of the sample ΔH_{smp} was obtained by the equation,

$$\Delta H_{\text{smp}} = \frac{A_{\text{smp}}}{A_{\text{std}}} \Delta H_{\text{std}} \quad (1)$$

where A_{smp} and A_{std} are the integrated areas for the sample and the standard, respectively and ΔH_{std} is the known enthalpy change of the standard between the initial and final temperatures [21]. The average heat capacity of the sample at the average temperature of the initial and final temperatures was obtained from the enthalpy change divided by the temperature increment.

In the low temperature region, the heat capacity of PH was measured by a thermal relaxation method using a PPMS (Quantum Design, Inc., USA) between 2 and 310 K. The amount of sample was 27.677 mg. The heat capacity data measured by this method were in good agreement with those obtained by DSC in the overlapped temperature region.

Results and discussion

The molar heat capacity of PT, PZ and PH obtained by DSC from room temperature up to 870 K are tabulated in Tables 1–3, respectively and plotted in Fig. 1. A peak is observed at 764 K in PT corresponding to the ferroelectric-paraelectric phase transition. PZ shows a peak at 504 K, that can be attributed to the antiferroelectric-paraelectric phase transition. There are two anomalies at 433 and 474 K in PH. These transition temperatures agree with the previous studies [1–3]. All the heat capacity curves approach asymptotically the classical limit value of Dulong–Petit law, that is 15R~124.7 J K⁻¹ mol⁻¹ (R is gas constant) in the case of simple perovskites, at high temperatures except for the transition temperature region.

To analyze the phase transition mechanism, the contribution due to the phase transition should be separated from the measured heat capacity. For this purpose, it is necessary the low-temperature heat capacity data are required to estimate the normal lattice contribution. As the low-temperature data had been measured by adiabatic calorimetry only on PT and PZ [20], the low-temperature heat capacity measurements were made on PH by a relaxation method. The results are given in Table 4. All the data are plotted in Fig. 2, where the lattice contribution denoted by solid lines was established by interpolating the normal heat capacity curves above and below the phase transition regions. The previous data of PT and PZ obtained by precise low-temperature adiabatic calorimetry [20] were compared with the present results, which were in good agreement in the overlapped temperature region between 300 and 420 K. The transition enthalpy ($\Delta_{\text{trs}}H$) and entropy ($\Delta_{\text{trs}}S$) calculated by subtracting the baseline from the measured heat capacity values are given in Table 5. The $\Delta_{\text{trs}}S$ of PT (7.3 J K⁻¹ mol⁻¹) is in good agreement with the previous studies (6.7 J K⁻¹ mol⁻¹ [1] and 8.6 J K⁻¹ mol⁻¹ [17]). On the other hand, $\Delta_{\text{trs}}S$ of PZ (9.9 J K⁻¹ mol⁻¹) was much larger than that of previous study (3.3 J K⁻¹ mol⁻¹ [2]). The present results of $\Delta_{\text{trs}}S$ of PT and PZ agrees with the values calculated according to the phenomenological thermodynamic theory (PT: 8.8 J K⁻¹ mol⁻¹, PZ: 6.1 J K⁻¹ mol⁻¹) [25, 26]. As the value of $\Delta_{\text{trs}}S$ of PH is very close to that of PZ, the mechanism of the

Table 1 Measured molar heat capacity of PbTiO₃ above room temperature (1 mol of PbTiO₃=303.07 g)

T/K	$C_p/\text{J K}^{-1} \text{mol}^{-1}$	T/K	$C_p/\text{J K}^{-1} \text{mol}^{-1}$	T/K	$C_p/\text{J K}^{-1} \text{mol}^{-1}$
303.7	103.7	498.6	120.4	693.8	134.5
308.6	104.2	503.6	120.7	698.8	134.2
313.5	104.6	508.6	121.7	703.8	135.7
318.4	105.3	513.6	122.0	708.9	137.2
323.4	106.0	518.6	122.3	713.9	137.8
328.3	106.5	523.6	122.6	718.9	138.6
333.3	107.1	528.6	122.9	723.9	140.1
338.3	107.8	533.6	123.2	728.9	140.9
343.3	108.1	538.6	123.5	733.9	142.6
348.3	108.9	543.7	123.8	738.9	144.8
353.3	109.3	548.7	124.1	743.9	147.5
358.3	109.7	553.7	124.4	749.0	150.7
363.3	110.3	558.7	124.7	754.0	157.0
368.3	110.7	563.7	124.7	759.0	177.5
373.3	111.2	568.7	124.9	763.9	406.7
378.4	111.7	573.7	125.7	768.9	152.5
383.4	112.2	578.7	125.6	773.8	125.8
388.4	112.6	583.7	125.5	778.8	123.9
393.4	113.1	588.7	125.3	783.7	123.0
398.4	113.5	593.7	126.2	788.7	122.6
403.4	113.4	598.7	125.7	793.7	122.4
408.4	113.9	603.7	125.7	798.7	122.3
413.4	114.3	608.7	126.1	803.7	122.2
418.4	113.9	613.7	126.5	808.6	121.9
423.5	114.3	618.7	126.5	813.6	121.9
428.5	114.7	623.7	126.8	818.6	121.8
433.5	115.2	628.7	127.2	823.6	121.8
438.5	115.4	633.7	127.4	828.6	121.8
443.5	115.9	638.8	128.2	833.5	121.6
448.5	116.1	643.8	129.1	838.5	121.9
453.5	116.4	648.8	129.3	843.5	122.1
458.5	117.0	653.8	129.1	848.5	122.4
463.5	117.4	658.8	130.3	853.5	122.1
468.5	117.8	663.8	130.5	858.5	122.1
473.6	118.1	668.8	130.6	863.5	122.0
478.6	118.4	673.8	130.6	868.4	122.3
483.6	118.7	678.8	132.0		
488.6	119.0	683.8	133.7		
493.6	120.2	688.8	135.2		

antiferroelectric phase transition of PH may be similar to that of PZ.

The ferroelectric phase transition in PT has been generally considered as a typical example of the displacive-type phase transition. In addition, the

mechanism of the antiferroelectric phase transition in PZ is also supposed to be of displacive-type. However, $\Delta_{\text{trs}}S$ associated with the phase transition mechanism is much larger than that of a conventional displacive-type phase transition. The large value of $\Delta_{\text{trs}}S$ may indicate

Table 2 Measured molar heat capacity of PbZrO₃ above room temperature (1 mol of PbZrO₃=346.42 g)

T/K	$C_p/\text{J K}^{-1} \text{mol}^{-1}$	T/K	$C_p/\text{J K}^{-1} \text{mol}^{-1}$	T/K	$C_p/\text{J K}^{-1} \text{mol}^{-1}$
303.7	109.6	498.5	191.5	693.7	117.6
308.5	110.2	503.5	261.1	698.7	117.8
313.4	110.9	508.5	150.6	703.7	117.3
318.4	111.4	513.5	133.6	708.7	115.8
323.3	112.1	518.5	127.3	713.7	117.6
328.3	112.6	523.5	124.0	718.7	117.9
333.3	113.4	528.5	122.0	723.7	117.3
338.2	113.8	533.6	120.9	728.6	117.4
343.2	114.5	538.6	120.0	733.6	117.5
348.2	115.1	543.6	119.2	738.6	118.1
353.2	115.6	548.6	118.9	743.6	118.3
358.3	116.1	553.6	118.2	748.6	118.4
363.3	116.7	558.6	118.1	753.6	119.2
368.3	117.1	563.6	117.7	758.5	119.0
373.3	117.7	568.6	117.7	763.7	119.1
378.3	118.3	573.6	117.7	768.7	119.0
383.3	118.8	578.6	117.6	773.8	118.1
388.3	119.3	583.7	118.0	778.8	118.3
393.3	119.9	588.7	118.0	783.8	118.0
398.3	120.6	593.7	118.1	788.8	117.3
403.3	120.4	598.7	118.5	793.7	118.1
408.3	120.9	603.7	118.5	798.7	118.0
413.4	121.6	608.7	117.9	803.7	118.2
418.4	121.6	613.7	118.2	808.7	118.0
423.4	122.2	618.7	118.3	813.6	118.5
428.4	122.8	623.8	118.1	818.6	117.9
433.4	123.6	628.8	119.0	823.6	117.9
438.4	124.2	633.8	118.1	828.6	118.1
443.4	125.0	638.8	117.9	833.6	118.4
448.4	125.8	643.8	118.1	838.6	118.0
453.4	126.4	648.8	118.3	843.5	118.2
458.4	127.3	653.8	117.6	848.5	117.9
463.5	128.2	658.8	117.8	853.5	118.3
468.5	129.2	663.8	119.0	858.5	118.0
473.5	130.7	668.8	118.2	863.5	118.0
478.5	132.3	673.8	117.9	868.5	118.6
483.5	134.5	678.8	118.5		
488.5	138.4	683.8	117.8		
493.5	146.4	688.7	117.5		

Table 3 Measured molar heat capacity of PbHfO₃ above room temperature (1 mol of PbHfO₃=433.70 g)

T/K	$C_p/\text{J K}^{-1} \text{mol}^{-1}$	T/K	$C_p/\text{J K}^{-1} \text{mol}^{-1}$	T/K	$C_p/\text{J K}^{-1} \text{mol}^{-1}$
303.0	108.9	498.8	119.5	694.2	121.1
307.9	109.7	503.8	119.3	699.2	117.6
312.8	110.4	508.8	119.2	704.1	118.1
317.8	111.1	513.8	119.1	709.1	118.0
322.8	111.9	518.9	119.0	714.1	118.3
327.7	112.7	523.9	119.0	719.1	118.2
332.7	113.4	528.9	119.2	724.0	117.8
337.8	114.2	533.9	119.1	729.0	119.4
342.8	114.9	539.0	119.1	734.0	118.2
347.8	115.5	544.0	119.1	739.0	118.1
352.8	116.2	549.0	119.0	744.0	118.3
357.9	116.9	554.0	119.0	748.9	118.3
362.9	117.5	559.0	119.0	753.9	118.3
367.9	118.2	564.0	119.0	758.9	118.2
372.9	118.9	569.1	119.0	763.8	118.6
378.0	119.5	574.1	119.0	768.8	118.7
383.0	120.3	579.1	118.9	773.8	118.7
388.1	121.1	584.1	118.2	778.8	118.8
393.1	122.0	589.1	118.1	783.8	118.6
398.1	122.4	594.1	118.1	788.7	118.7
403.1	123.8	599.1	117.3	793.7	119.0
408.2	124.7	604.1	118.0	798.7	118.6
413.2	125.7	609.1	117.4	803.7	118.8
418.3	127.5	614.1	117.4	808.7	118.7
423.3	129.3	619.1	117.4	813.6	118.7
428.3	137.8	624.1	117.5	818.6	118.9
433.4	189.5	629.1	117.3	823.6	118.3
438.4	130.6	634.1	117.4	828.6	118.6
443.4	130.2	639.1	117.3	833.6	118.9
448.5	131.6	644.2	117.5	838.5	118.7
453.5	133.3	649.2	117.4	843.5	118.2
458.5	135.5	654.2	117.6	848.5	118.4
463.5	139.8	659.2	117.8	853.5	118.3
468.6	151.7	664.2	117.6	858.5	118.6
473.6	283.5	669.2	117.5	863.5	118.6
478.6	141.3	674.2	118.2	868.5	118.4
483.7	123.1	679.2	118.0		
488.7	120.4	684.2	118.2		
493.7	119.9	689.2	119.2		

Table 4 Measured molar heat capacity of PbHfO₃ below room temperature (1 mol of PbHfO₃=433.70 g)

T/K	$C_p/\text{J K}^{-1} \text{mol}^{-1}$	T/K	$C_p/\text{J K}^{-1} \text{mol}^{-1}$	T/K	$C_p/\text{J K}^{-1} \text{mol}^{-1}$
2.033	0.00176	7.241	0.3147	25.67	13.27
2.098	0.00230	7.481	0.3635	26.50	13.95
2.178	0.00253	7.729	0.4195	27.40	14.66
2.251	0.00280	7.982	0.4818	28.32	15.39
2.326	0.00314	8.244	0.5546	29.26	16.11
2.406	0.00341	8.517	0.6360	30.23	16.87
2.481	0.00370	8.799	0.7266	31.22	17.65
2.563	0.00425	9.086	0.8277	32.25	18.44
2.648	0.00477	9.386	0.9410	33.32	19.24
2.732	0.00521	9.697	1.069	34.42	20.07
2.819	0.00585	10.01	1.208	35.56	20.92
2.910	0.00651	10.34	1.360	36.75	21.79
3.010	0.00737	10.68	1.528	37.96	22.66
3.107	0.00830	11.04	1.712	39.22	23.55
3.212	0.00923	11.40	1.913	40.52	24.45
3.316	0.0103	11.78	2.129	41.86	25.40
3.428	0.0115	12.16	2.367	43.24	26.38
3.539	0.0132	12.57	2.618	44.66	27.38
3.654	0.0146	12.99	2.894	46.14	28.40
3.784	0.0171	13.42	3.190	47.66	29.44
3.913	0.0195	13.86	3.503	49.23	30.53
4.041	0.0221	14.32	3.839	50.76	31.56
4.171	0.0258	14.79	4.195	51.89	32.30
4.308	0.0295	15.28	4.568	53.59	33.37
4.448	0.0336	15.77	4.962	55.10	34.33
4.594	0.0393	16.30	5.392	55.87	35.01
4.747	0.0456	16.83	5.827	56.63	35.29
4.900	0.0526	17.40	6.302	58.13	36.22
5.061	0.0609	17.98	6.791	59.66	37.14
5.228	0.0702	18.57	7.286	61.16	38.02
5.400	0.0815	19.18	7.805	62.68	38.96
5.579	0.0942	19.80	8.344	64.20	39.89
5.763	0.1099	20.44	8.882	65.71	40.85
5.954	0.1280	21.12	9.452	67.21	41.77
6.146	0.1482	21.82	10.06	68.72	42.67
6.355	0.1744	22.54	10.67	70.24	43.59
6.567	0.2001	23.28	11.28	71.76	44.49
6.781	0.2337	24.05	11.91	73.26	45.40
7.009	0.2712	24.85	12.58	74.79	46.29
76.30	47.15	133.8	73.37	205.3	93.27
77.82	47.88	135.3	73.91	207.4	93.76
79.34	48.73	136.9	74.42	209.4	94.32
80.85	49.51	138.4	74.99	211.4	94.61

Table 4 Continued

T/K	$C_p/\text{J K}^{-1} \text{mol}^{-1}$	T/K	$C_p/\text{J K}^{-1} \text{mol}^{-1}$	T/K	$C_p/\text{J K}^{-1} \text{mol}^{-1}$
82.37	50.35	139.9	75.52	213.4	95.08
83.89	51.15	141.4	76.06	215.4	95.40
85.41	51.98	142.9	76.56	217.4	95.93
86.92	52.76	144.4	77.06	219.4	96.39
88.45	53.54	145.9	77.57	221.4	96.69
89.95	54.36	147.4	78.02	223.4	97.12
91.47	55.09	148.9	78.48	225.4	97.60
92.99	55.85	150.5	78.95	227.4	97.81
94.50	56.58	152.0	79.50	229.4	98.08
96.02	57.33	153.5	79.99	231.4	98.65
97.52	58.09	155.6	80.67	233.4	98.94
99.05	58.75	157.4	81.20	235.4	99.26
100.6	59.59	159.4	81.84	237.4	99.59
102.1	60.24	161.4	82.42	239.4	100.1
103.6	61.00	163.4	83.07	241.4	100.4
105.1	61.68	165.4	83.57	243.4	100.6
106.6	62.35	167.4	84.13	245.5	101.1
108.2	63.06	169.4	84.60	247.5	101.4
109.7	63.67	171.4	85.13	249.5	101.7
111.2	64.35	173.4	85.70	251.4	102.1
112.7	65.01	175.4	86.22	253.5	102.3
114.2	65.65	177.4	86.75	255.5	102.6
115.7	66.31	179.4	87.20	257.4	103.0
117.2	66.91	181.4	87.58	259.5	103.3
118.7	67.55	183.4	88.14	261.5	103.4
120.2	68.17	185.4	88.66	263.5	103.4
121.8	68.74	187.4	89.15	265.4	104.4
123.3	69.39	189.4	89.64	267.5	104.5
124.8	70.01	191.4	90.05	269.5	104.6
126.3	70.59	193.4	90.59	271.4	105.1
127.8	71.20	195.4	91.10	273.5	105.3
129.3	71.75	197.4	91.63	275.5	105.3
130.8	72.26	199.4	91.97	277.5	105.9
132.3	72.82	201.4	92.46	279.5	106.0
76.30	47.15	203.4	92.98	281.5	106.3
283.5	106.5	293.5	108.0	303.4	109.5
285.4	106.9	295.4	108.4	305.5	109.6
287.5	107.3	297.4	109.0	307.4	109.9
289.5	107.4	299.4	109.4	309.4	109.7
291.5	107.8	301.5	109.5	311.4	110.0

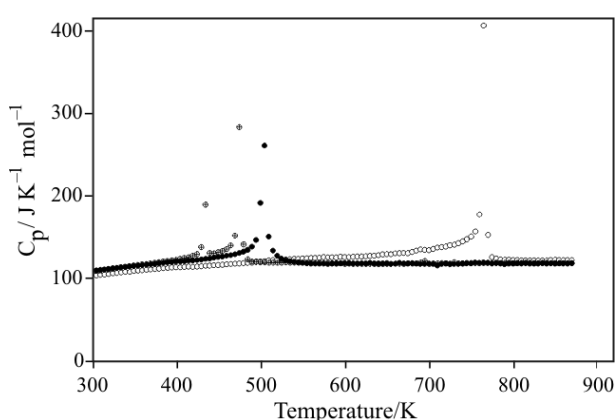


Fig. 1 Measured heat capacity C_p in the range temperature 300–870 K. ○ – PbTiO_3 (PT), ● – PbZrO_3 (PZ), ⊕ – PbHfO_3 (PH)

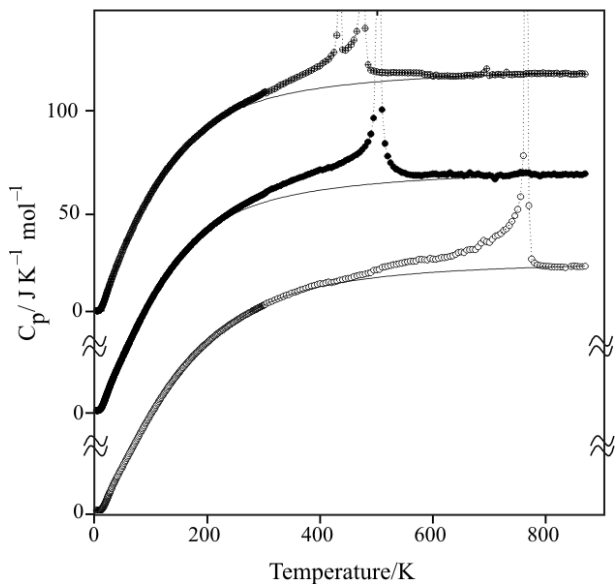


Fig. 2 Measured molar heat capacity C_p in the range temperature 2–870 K. ○ – PbTiO_3 (PT), ● – PbZrO_3 (PZ), ⊕ – PbHfO_3 (PH) Solid lines denote the estimated lattice contribution (see text)

Table 5 Thermodynamic properties of the phase transitions in PbMO_3 ($M=\text{Ti}, \text{Zr}$ and Hf)

	T_{trs}/K	$\Delta_{\text{trs}}H/\text{kJ mol}^{-1}$	$\Delta_{\text{trs}}S/\text{J K}^{-1} \text{mol}^{-1}$
PbTiO_3	764	4.9	7.3
PbZrO_3	504	4.4	9.9
PbHfO_3	433, 474	4.0	9.3

an order-disorder-type mechanism. In recent years, an order-disorder character of the ferroelectric and/or antiferroelectric phase transition in PbMO_3 has also been found by several studies [7, 10–16]. Consequently, the phase transition mechanism of the present three compounds may be explained to some extent assuming an order-disorder-type mechanism.

Conclusions

Heat capacity measurements on PbMO_3 ($M=\text{Ti}, \text{Zr}$ and Hf) were carried out above room temperature using DSC with enthalpy method. Heat capacity of PH was also measured below room temperature using PPMS. The present results on PT and PZ showed good agreement with the previous data measured by an adiabatic method in the overlapped temperature region. The large value of $\Delta_{\text{trs}}S$ implies an order-disorder-type mechanism of the phase transitions in PT, PZ and PH.

References

- G. Shirane and E. Sawaguchi, Phys. Rev., 81 (1950) 458.
- G. Shirane, E. Sawaguchi and A. Tanaka, Phys. Rev., 80 (1950) 485.
- G. Shirane and R. Pepinsky, Phys. Rev., 91 (1953) 812.
- G. A. Samara, Phys. Rev. B, 1 (1970) 3777.
- D. L. Corker, A. M. Glazer, W. Kaminsky, R. W. Whatmore, J. Dec and K. Rolder, Acta Cryst., Sect., B54 (1998) 18.
- V. Madigou, J. L. Baudour, F. Bouree, Cl. Favotto, M. Roubin and G. Nihoul, Philos. Mag., A79 (1999) 847.
- Y. Kuroiwa, H. Fujiwara, A. Sawada, H. Kawaji and T. Atake, J. Korean Phys. Soc., 46 (2005) 296.
- G. Shirane, J. D. Axe, J. Harada and J. P. Remeika, Phys. Rev. B, 2 (1970) 155.
- G. Burns and B. A. Scott, Phys. Rev. B, 7 (1973) 3088.
- M. D. Fontana, K. Wojcik, H. Idrissi and G. E. Kugel, Ferroelectrics, 107 (1990) 91.
- R. J. Nelmes, R. O. Piltz, W. F. Kuhs, Z. Tun and R. Restori, Ferroelectrics, 108 (1990) 165.
- N. Sicron, B. Ravel, Y. Yacoby, E. A. Stern, F. Dogan and J. J. Rehr, Phys. Rev. B, 50 (1994) 13168.
- T. Miyanaga, D. Diop, S. Ikeda and H. Kon, Ferroelectrics, 274 (2002) 41.
- K. Rolder, M. Maglione, M. D. Fontana and J. Dec, J. Phys. Condens. Matter, 8 (1996) 10669.
- S. Aoyagi, Y. Kuroiwa, A. Sawada, H. Tanaka, J. Harada, E. Nishibori, M. Takata and M. Sakata, J. Phys. Soc. Jpn., 71 (2002) 2353.
- Y. Kuroiwa, H. Fujiwara, A. Sawada, S. Aoyagi, E. Nishibori, M. Sakata, M. Takata, H. Kawaji and T. Atake, Jpn. J. Appl. Phys., 43 (2004) 6799.

- 17 V. G. Bhide, M. S. Hegde and K. G. Deshmukh, *J. Am. Ceram. Soc.*, 51 (1968) 565.
- 18 J. P. Remeika and A. M. Glass, *Mater. Res. Bull.*, 5 (1970) 37.
- 19 G. A. Rossetti Jr. and A. Navrotsky, *J. Solid State Chem.*, 144 (1999) 188.
- 20 Y. Moriya, T. Tojo, H. Kawaji and T. Atake (to be published).
- 21 S. C. Mraw and D. F. Naas, *J. Chem. Thermodyn.*, 11 (1979) 567.
- 22 H. K. Cammenga, W. Eysel, E. Gmelin, W. Hemminger, G. W. H. Höhne and S. M. Sarge, *Thermochim. Acta*, 219 (1993) 333.
- 23 S. M. Sarge, E. Gmelin, G. W. H. Höhne, H. K. Cammenga, W. Hemminger and W. Eysel, *Thermochim. Acta*, 247 (1994) 129.
- 24 National Institute of Bureau and Standards Certificate, Standard Reference Material 720, Synthetic Sapphire (α -Al₂O₃).
- 25 M. J. Haun, E. Furman, S. J. Jang, H. A. McKinstry and L. E. Cross, *J. Appl. Phys.*, 62 (1987) 3331.
- 26 M. J. Haun, T. J. Harvin, M. T. Lanagan, Z. Q. Zhuang, S. J. Jang and L. E. Cross, *J. Appl. Phys.*, 65 (1989) 3173.

Received: May 6, 2008

Accepted: August 26, 2008

DOI: 10.1007/s10973-008-9220-y